Int. J. Electrochem. Sci., 8 **(2013)** 5738 - 5754

International Journal of
ELECTROCHEMICAL
SCIENCE
www.electrochemsci.org

Electrochemical Characterization of Multi-walled Carbon Nanotubes/ Polyvinyl Alcohol Coated Electrodes for Biological Applications

Wei Li[1], *Yudong Zheng*[1,*], *Xiaoli Fu*[1], *Jiang Peng*[2], *Lingling Ren*[3], *Pengfei Wang*[1],*Wenhui Song*[4]

[1]School of Materials Science and Engineering, University of Science and Technology Beijing, Beijing 100083, PR China
[2] Institute of Orthopaedics，Chinese PLA General Hospital，Beijing 100853
[3] National Institute of Metrology of China, Beijing, 100013,PR China
[4] Wolfson Center for Materials Processing,School of Engineering and Design, Brunel University, London UB8 3PH, UK
[*]E-mail: zhengyudong@mater.ustb.edu.cn

Received: 30 October 2012 / *Accepted:* 21 November 2012 / *Published:* 1 April 2013

A multi-walled carbon nanotubes (MWCNTs)/polyvinyl alcohol (PVA) composite coating modified electrode with excellent microstructural homogeneity was produced from aqueous suspensions using electrophoretic deposition (EPD). The zeta-potential of MWCNTs/PVA composite particles near electrodes plays a vital importance on the process of electrophoretic deposition, for the decrease of zeta-potentials leads to particle coagulation. The effect of main EPD parameters including applied voltage and deposition time on the deposit yield as well as the electrochemical performance of modified electrode was investigated. At the optimal EPD condition (voltage of 35v and deposition time of 2.5 min). MWCNTs/PVA modified electrodes showed well-defined voltammetric responses for the Fe (CN) $_6^{4-}$/ Fe (CN) $_6^{3-}$ redox system in phosphate buffer solution (PBS). Both anodic and cathodic peak currents of modified electrode exceed those of bare copper electrode, which means modified electrode delivers higher charge. The peak currents depended linearly on the square root of the scan rate in the range of 10mv/s-100mv/s, suggesting diffusion-control and fast electron conduction within MWCNTs/PVA composite coating.

Keywords: Electrophoretic deposition, Composite coating, Cyclic Voltammetry, Multi-walled Carbon Nanotubes , Polyvinyl Alcohol

1. INTRODUCTION

Electrophoretic deposition (EPD) has attracted substantial attention for the fabrication of thin films and coatings of polymers[1], carbon nanotubes (CNTs)[2, 3] and composite materials [4-6] for

the surface modification. Compare to other methods, EPD offers the advantage of a high deposition rate and the possibility of the fabrication of relatively thick coatings [7, 8]. EPD mechanism involves the electrophoretic motion of charged particles and coating formation at the electrode surface under the influence of an electric field[9]. EPD enables the formation of uniform coatings on substrate having complex shape and large surface area. Moreover, this method allows the formation of composite and multi-layer coatings, containing polymers and inorganic nanoparticles [5, 10, 11].

Carbon nanotubes (CNTs) show unique structural, electronic and mechanical properties and they have been used in applications of biosensors for a long time [12-14]. When CNTs are used as electrode materials, the electroactive ends of the CNTs can be exploited to controllably deliver charge out of a nano- or micrometer-long channel, and the ballistic conductance guarantees there will be no shortage of electrons at that site[15]. Numerous advantages of CNTs as electrode materials have been attested for detection of diversified biomolecules, especially for the detection of glucose and neurotransmitters.

Britto was the first to use carbon nanotube electrodes to examined the oxidative behavior of dopamine, and he found ideal reversibility in cyclic voltammetry of two-electron oxidation of dopamine to dopaminequinone[16]. Hill O observed reproducible, well-behaved voltammetric responses of redox proteins on carbon nanotube electrode[17]. Giuseppe Palleschi constructed paste electrodes using single-wall carbon nanotubes mixed with mineral oil, and compared electrochemical behavior of this kind of electrode with that of graphite paste electrodes[18]. Yu-Chen Tsai dropped MWCNTs-PVA aqueous solution onto the surface of glassy carbon electrode, and well-defined voltammetric responses are observed for the $Fe(CN)_6^{4-}$/ $Fe(CN)_6^{3-}$ redox system[19].

As the carbon nanotubes are being extensively explored for various applications, evaluation of those nanomaterials is of extremely important. One of the greatest concerns about toxicity effects of CNT is their risk in the body environment, such as inflammatory responses or the formation of granuloma[20]. To avoid such adversity, we incorporate Poly (vinyl alcohol) (PVA) hydrogel molecules with CNTs to get rid of the shedding of CNTs. PVA is a useful water-soluble synthetic hydrogel, which has been widely studied and applied in the form of fiber, film and gel[21-23]. PVA hydrogel has been advanced as a biomaterial for the applications of medical devices like biosensor and membranes with selective permittivity, because of its viscoelastic nature, high water content, non-toxic and biocompatibility [24, 25]. Compare to other hydrogel molecules such as hyaluronic acid [26] and chitosan [27], PVA is easy to get crosslinked without the addition of chemical crosslinking agents, which may be devastating when released into the body system. After a freezing-thawing process, PVA molecular chains are cross-linked by entanglement, molecular association, or crystallites [19, 28].Our research group has reported the co-electrophoretic deposition of both MWCNTs and PVA under alternating current[29]. Stable dispersion of MWCNTs/PVA in deionized water was prepared using two common surfactants: cetrimonium bromide and sodium dodecyl benzene sulfonate. But the kinetics of EPD has not been investigated and how exactly different factors like voltage and time working on the deposition process is still unknown.

In this article, we have demonstrated another successful way to disperse MWCNTs within PVA aqueous solution by functionalizing the nanotubes with strong oxidant and co-deposit them on the surface of bare copper electrode under direct current to form a uniform coating. The particle

coagulation mechanism during the EPD process has been studied and the formation of deposit by electrophoretic deposition could be explained by the variation of zeta-potential during the process. The effect of EPD parameters, such as deposition time and applied voltage on deposit yield and electrochemical performance, as well as the voltammetric responses of the newly develop electrodes against bare copper electrode under the same conditions have also been investigated.

2. MATERIALS AND METHODS

2.1 Reagents

MWCNTs (diameter~40–60 nm, length~1–2μm, amorphous <3%) were purchased from Shenzhen Nanotech Port Co. Ltd. in China and used as received. Polyvinyl alcohol powders (polymerization degree of ~1750 and 99% hydrolyzed) were supplied by Beijing Xisi Chemicals Co. Ltd. and used as received to prepare 0.5 wt.% aqueous solutions. K_3 [Fe (CN) $_6$] was supplied by Beijing Chemical Works. Water was distilled and deionized. All other reagents were of analytical-reagent grade and used without further purification.

2.2 Preparation of MWCNTs/PVA suspension for EPD

0.5g of raw MWCNTs was put in 180 mL of 30% H_2O_2 subjected to 30 min ultrasonic wave, and was refluxed at 80℃ for 2 hours. The MWCNTs aggregates were obtained by a mild centrifugation (CF) step for 40 min at 7000 rpm followed by decantation of the supernatant. After CF, the MWCNTs were treated at elevated temperature and prepared by chemical oxidation in a concentrated HNO_3 and H_2SO_4 solution (1:3 volume ratios). Once cooling, the oxidized MWCNTs were washed to neutral with distilled water.

50mg of MWCNTs after oxidization were mixed with 50g distill water to get a stable black aqueous solution (1mg/mL) subjected to ultrasonic wave for 2 hours. As for obtaining the MWCNTs/PVA dispersion, add 250mg PVA into the MWCNTs aqueous solution mentioned above and heat up to 90℃ and maintained for 1.5h. The concentration of MWCNTs is 1mg/mL, and the weight ratio of PVA is 0.5wt%. This kind of mixed suspension was ultrasonicated for about 50 min just before the EPD experiments.

Infrared spectra (FTIR spectra) of pristine MWCNTs and acid-treated MWCNTs were tested using a FT-IR spectrometer (Perkin-Elmer, model spectrum one). FTIR spectra were obtained in a range of frequency from 4000 $cm^{-1}$to 450 cm^{-1} with a resolution of 4 cm^{-1}.

A stable and homogeneous suspension is a prerequisite for successful EPD. In the case of good dispersion, multi-walled nanotubes have negative charge and are cut short, and the stability is high. In the opposite case, agglomerates settle fast in a poor dispersion[30]. Homogeneity of the dispersions was measured using an OPTEC BK300 optical microscope.

Zeta-potential (ζ-potential) of the particles has a great influence on the stability of suspension and the ζ-potential of MWCNTs and MWCNTs/PVA particles were tested using a Zeta Potential and Submicron Particle Size Analyzer (Delsa TM Nano C).

2.3 Electrophoretic deposition

EPD was carried out using a DC power supply (DYY-6C, BEIJING LIUYI INSTRUMENT FACTORY, Beijing, China) under a range of conditions, including variation of electric field strength (between 10 V/cm and 45 V/cm) and deposition time (from 0.5 to 4.5min.), in order to investigate the kinetics of the deposition process and the optimal condition. All the electrophoretic deposition experiments were performed at room temperature. Both electrodes in the EPD cell were copper foils (10 mm*10 mm*0.2 mm) fixed parallel to each other at a constant distance (1 cm) and a DC voltage was applied. Once the deposition is finished, the coated copper electrode was taken out carefully vertically along with the substrate to avoid any drag between the wet coating and the remaining suspension. The MWCNTs/PVA coated electrode was placed into a refrigerator and kept at -26℃ for 10 h and then it was allowed to thaw at room temperature for 4 h and repeated the whole process for four times. Weigh both kinds of electrodes to determine the deposit yield and the products were ready for characterization.

2.4 Characterization of modified electrodes

The surface morphology of MWCNTs/PVA modified electrodes was characterized by field emission gun-scanning electron microscopy (FESEM, Apollo 300, and 10 KV). Cyclic voltammetry was performed using the electrochemical workstation CH instrument 618D with a conventional three-electrode system, a working electrode, a platinum plate (20 mm*20 mm*0.3 mm)as counter electrode and a saturated calomel electrode(SCE) as reference electrode. The chemical composition of the PBS solution is $Na_2HPO_4 \cdot 12H_2O$ (10.5 g/L) and KH_2PO_4 (2.6 g/L).

3. RESULTS AND DISCUSSION

3.1 Pre-treatment of MWCNTs before EPD

It is well known that pristine MWCNTs often aggregate or entangle and are difficult to disperse well in aqueous solution due to the hydrophobic nature of graphene wall surface, large specific surface area, high surface energy and weak van der Waals forces among MWCNTs[31]. Typically, a mixture of concentrated nitric and sulphuric acids is used to cut the tubes into small ones and introduces carboxylic and other oxygen-containing groups at the defects of the tube, so as to electrostatically stabilize the MWCNTs in water by developing a negative surface charge[32, 33]. The FTIR results presented in Fig. 1 show that the functional groups, including carbonyl groups (C=O, 1718cm^{-1}, v(C-O),1196cm^{-1}), hydroxyl groups (-OH, 3400cm^{-1}) formed on the as-MWCNTs surface[34]. Optical images of the acid-treated MWCNT (a-MWCNTs) aqueous dispersion and a-MWCNTs/PVA dispersion were taken to further prove the effectiveness of oxidization and homogeneity of the solution (Fig. 2). At micron-scale resolution, nanotube agglomerates became visible in pristine MWCNTs (p-

MWCNTs) solution and p-MWCNTs/PVA aqueous dispersion within a few hours. In the meantime, a-MWCNTs and a-MWCNTs/PVA dispersion appeared to be uniform and stable after 48h.

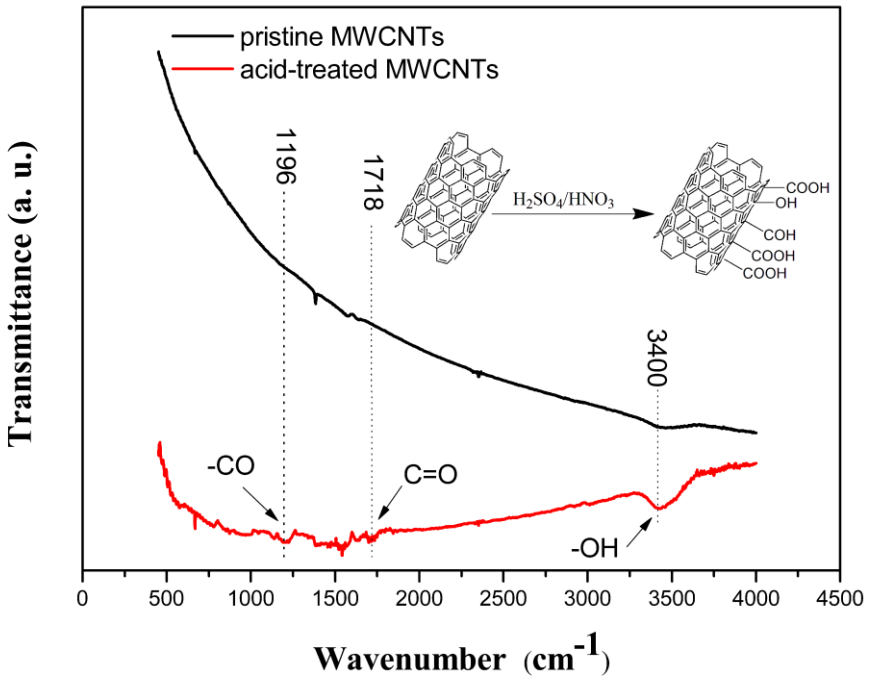

Figure 1. FTIR spectra of pristine MWCNTs and acid-treated MWCNTs.

particles	5 min after sonication	48 hour after sonication
P-MWCNTs	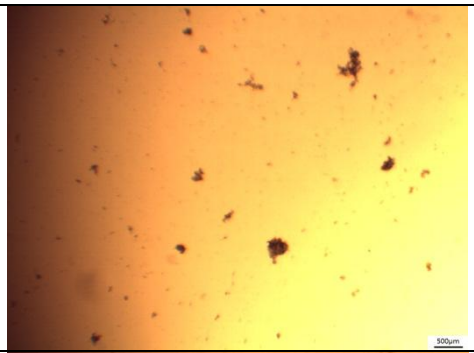	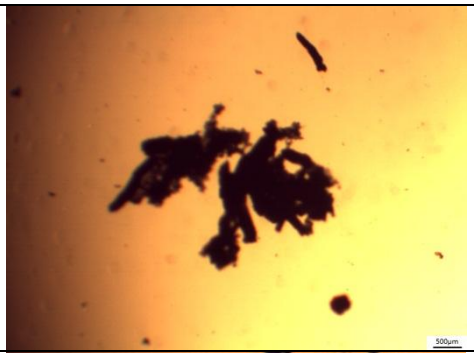
p-MWCNTs/PVA	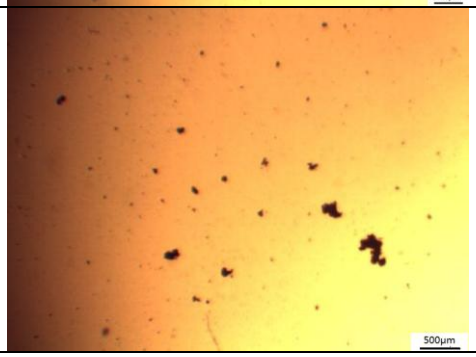	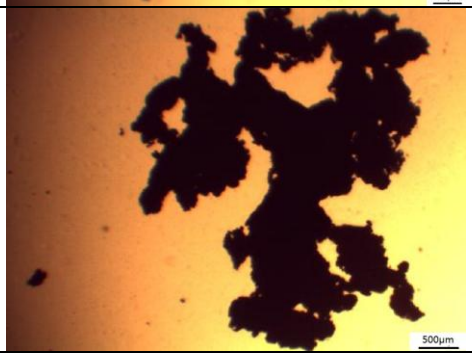

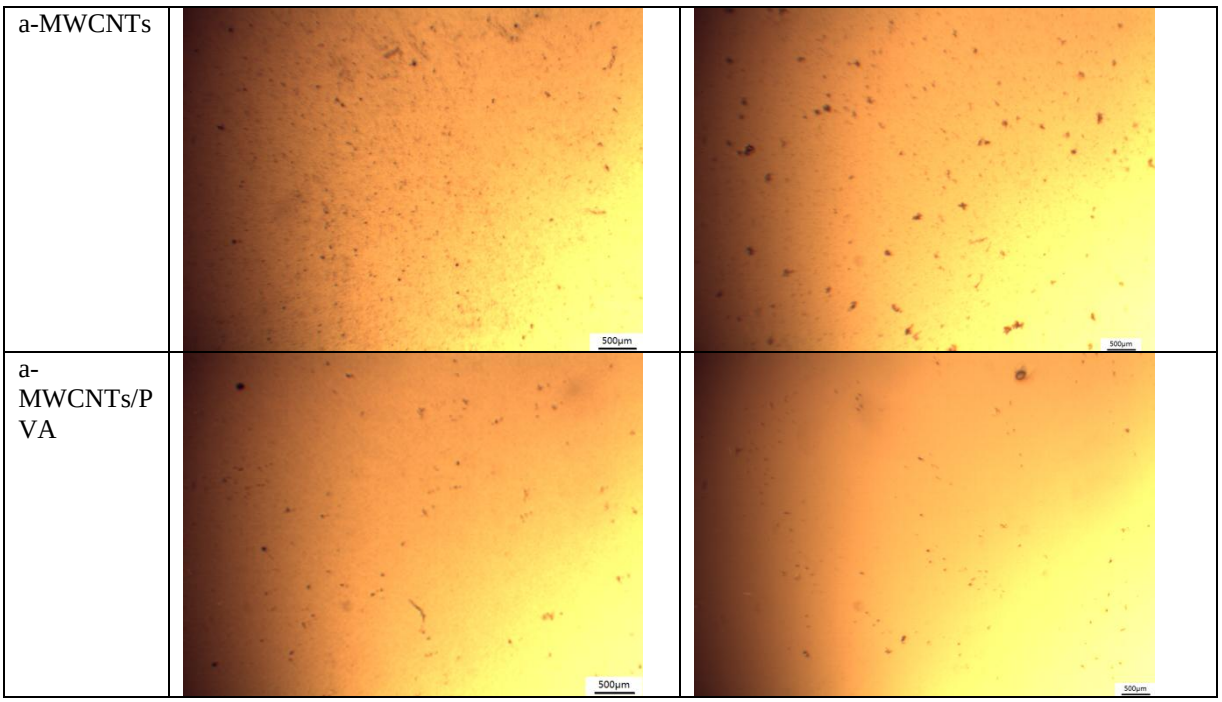

Figure 2. Transmitted optical images of the p-MWCNTs, p- MWCNTs/PVA, a- MWCNTs, and a-MWCNTs/PVA aqueous dispersions (1 mg/mL) taken at different time.

3.2 Influence of different parameters on EPD process

EPD is achieved via the motion of charged particles, dispersed in a suitable solvent, towards an electrode under an applied electric field. Preparation of a stable dispersion of particles in a suitable solvent where the particle surface has a high zeta-potential (ζ-potential) is a necessary prerequisite for successful EPD. EPD is essentially a two-step process. In the first step, particles suspended in a liquid are forced to move towards an electrode by applying an electric field (electrophoresis). In the second step, the particles accumulate at the electrode and form a coherent and rigid deposit at the relevant electrode (deposition). Deposition occurs only on conducting surfaces[35]. It is worth noting that the parameterζ-potential , applied voltage and deposit time during the EPD process may affect the deposition of MWCNTs/PVA.

3.2.1 Effect of zeta-potential on coagulation mechanism

The zeta potential (ζ-potential), reflecting the surface charge of on the colloid, has implications of stability of the dispersions. The higher theζ-potential is, the more stable the dispersions will be. With oxygen-containing groups introduced on the wall and the end of the nanotubes, very highly negative charged MWCNTs are obtained by using mixed acids, whereas the pristine MWCNTs are almost neutral. This negative charge leads to electrostatic repulsion between the nanotubes, and this stabilizes the dispersion even when PVA molecules are absorbed on the surface of the nanotubes.

The zeta values are calculated from the particle velocities with method of the Helmholtz-Smoluchowski equation[36],

$$\xi = 4\pi\mu\eta / D \quad (1)$$

Where μ is the electrophoretic mobility and ηand D are respectively the viscosity and the dielectric constant of the liquid[37]. ζ-potential of the p-MWCNTs, a-MWCNTs, p-MWCNTs/PVA and a-MWCNTs/PVA dispersions as a function of pH are given in Fig.3. It is clear that the a-MWCNTs and a-MWCNTs/PVA composite particles are negatively charged. For a-MWCNTs dispersion, the maximum zeta potential is as low as -48.8 mv. A decrease of the value is caused by the absorption of PVA molecular chains on the surface of carbon nanotubes for almost all pH values, but the maximum zeta potential is a guarantee for the stability of the dispersion and the success of EPD. While for p-MWCNTs and p-MWCNTs/PVA dispersions, the values of ζ-potential are comparatively small at a large scale of pH, and the nanotubes are easy to aggregate and settle down.

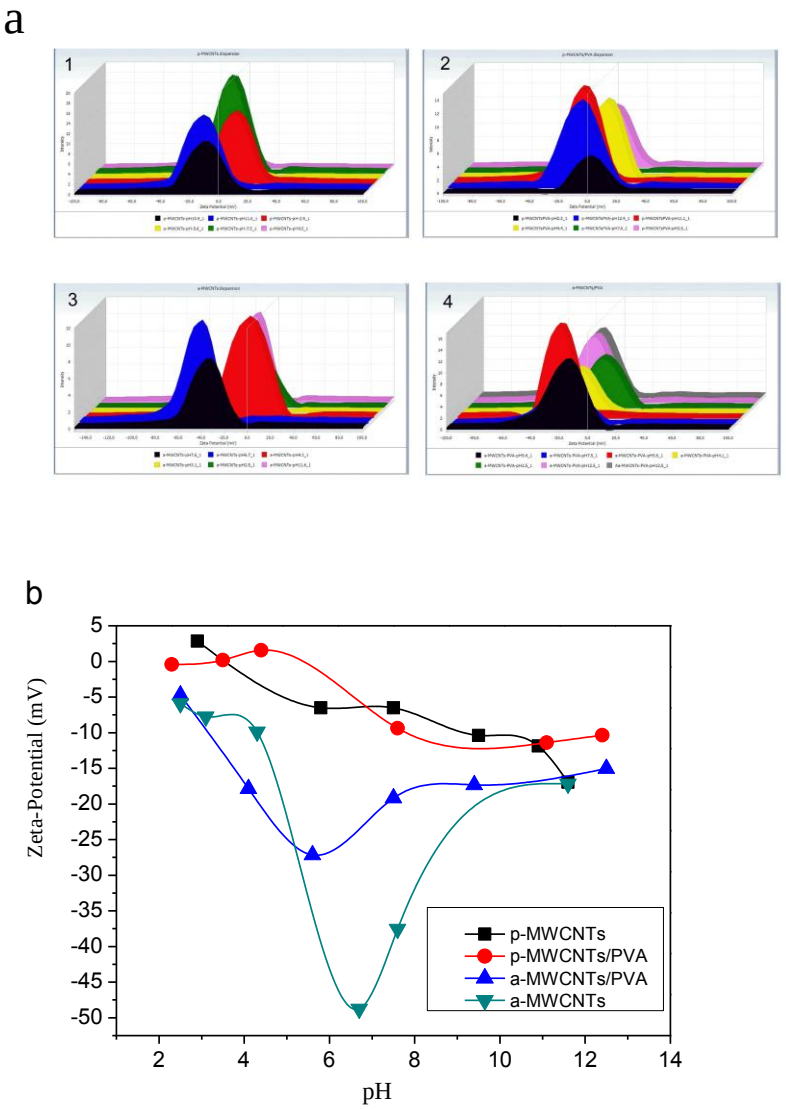

Figure 3 (a) The ζ-potential distribution 3D curves for different kinds of dispersions. (1) p-MWCNTs dispersion ;(2) p-MWCNTs/PVA dispersion ;(3) a-MWCNTs dispersion ;(4) a-MWCNTs/PVA dispersion. (b) Plot of the ζ-potential of p-MWCNTs, a-MWCNTs, p-MWCNTs/PVA, and a-MWCNTs/PVA as a function of the pH.

Since the negatively charged a-MWCNTs/PVA, it should be noted that the EPD happened on anode copper. The composite particles are brought to the anode by electrophoresis, and they would neutralize and become static once getting contact to the electrode[38]. Apart from the charge neutralization, other reason may explain the formation of deposit. As Zhitomirsky pointed, the zeta-potential lowering is also a factor for EPD[39]. With the hydrolysis of water, the local pH near the anode is expected to decrease. Similarly, the evolution of H_2 at the cathode/solution interface will decrease the concentration of H^+. So an increase in pH is expected at the cathode/solution interface (Fig. 4). The charge transfer process involves is shown below:

$$2H_2O + 2e^- \rightarrow 2OH^- + H_2\uparrow$$
$$2H_2O - 4e^- \rightarrow 4H^+ + O_2\uparrow \quad (2)$$

As the local pH decreases near the anode, the ζ-potential value reduced and then the surface charge reduced. So the strong repulsive force among the particles became weak, the suspension will spontaneously coagulate because of strong van der Waals attraction forming the deposit on the anode.

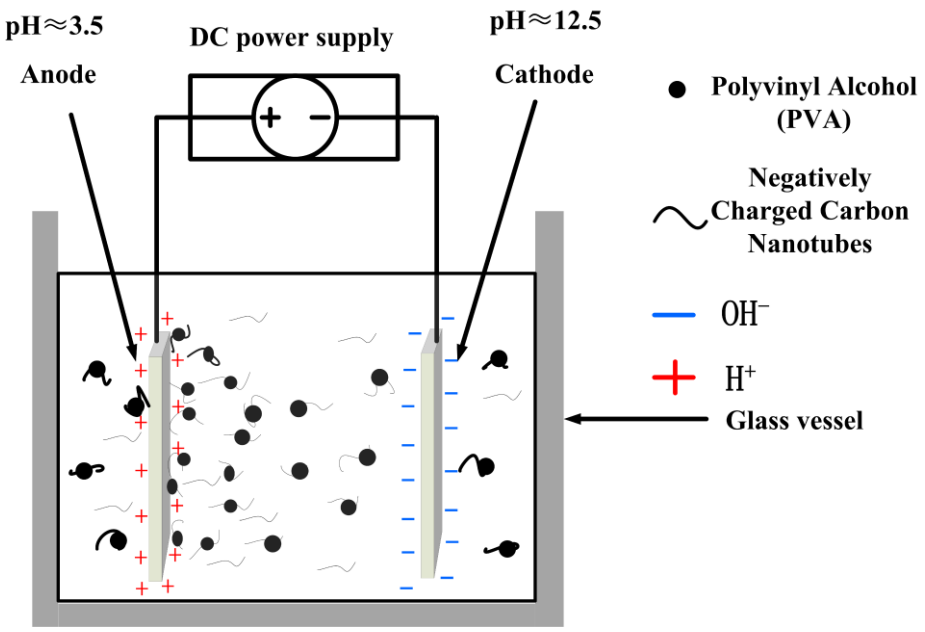

Figure 4. Schematic diagram of anodic-electrophoretic deposition of MWCNTs/PVA. The local pH changing during the electrophoretic process as a result of the electrolysis of water.

3.2.2 Effect of voltage on deposit yield and electrochemical performance

The kinetics of electrophoretic deposition was first derived by Hamaker by applying the principle of conservation of mass[40, 41].The relation between the deposit weight, W, and the electric field intensity, E, can be described as follows:

$$Hamaker\ equation: w = \int_{t_1}^{t_2} \mu.E.A.C.dt \quad (3)$$

Where μ is electrophoretic mobility, E is field strength, A is the surface area of the electrode, C is the particle mass concentration in suspension and t is time. Therefore, the amount of the deposited material can be controlled by varying the parameters such as applied voltage and deposit time. In this study, we investigate how these parameters affect the deposit yield and the electrochemical performance of electrodes.

The deposit yield (deposit weight per surface area) was measured at different voltage (10, 15, 20, 25, 30, 35, 40 and 45 V) and constant time (1 min). The deposit yield versus applied voltage (Y-V) curve in Figure 5(a) shows that the deposit yield increases with increasing the applied voltage， which is in agreement with equation (3). It means as the electric-field strength increases (the distance between electrodes are fixed), the movement of MWCNTs/PVA is faster. It could also be manifested in Figure 5(b) that the higher voltage, the more MWCNTs/PVA composite nanoparticles deposited on the substrate. The relationship between MWCNTs/PVA deposition yield and voltage for EPD matches the results observed by other researchers [39, 42].

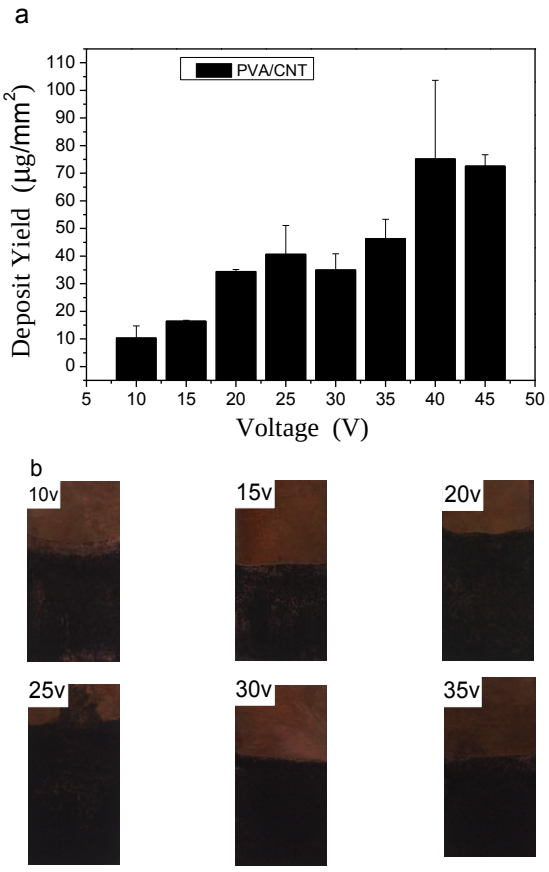

Figure 5. (a) Deposit yield versus applied voltage for composite film prepared for 1 min from MWCNTs/PVA dispersions (electrode separation=1cm). (b) Optical photographs of MWCNTs/PVA composite coating obtained by EPD at different voltages, ranging from 10v to 35v. As voltage increasing, deposit yield increases.

The surface morphology of different kinds of MWCNTs/PVA modified electrodes corresponding to varied applied potentials is shown in Fig 6. It is evident that as the voltage becomes higher, the amount of MWCNTs/PVA increases accordingly, and the deposition film tends to uniform and even. But for higher voltage (above 45 v), more and more bubbles were found near the surface of two electrodes as the electrolysis of water, and it is difficult to get uniform deposition.

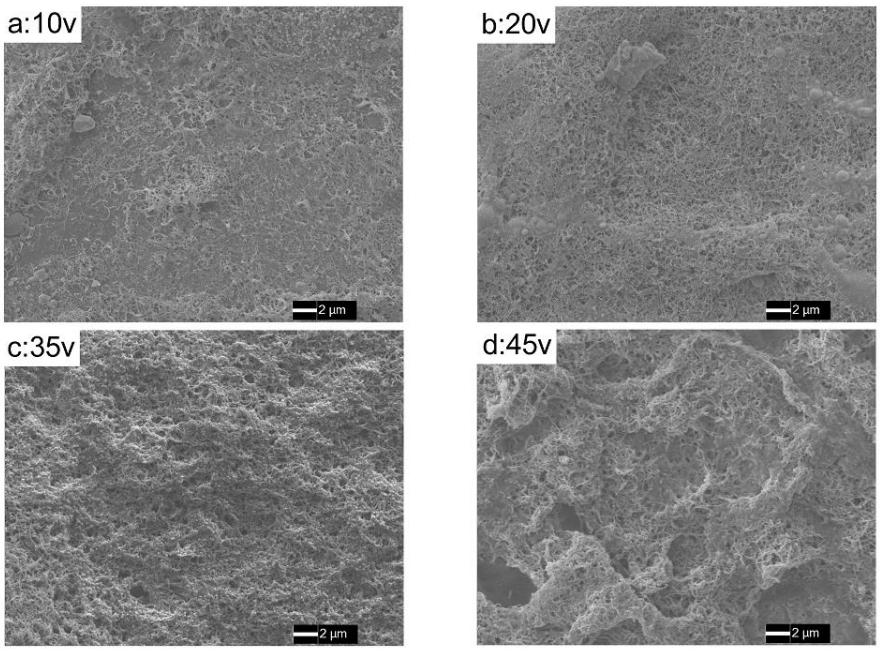

Figure 6. Surface morphology of deposits obtained by EPD (a) at an applied voltage of 10v, (b) at an applied voltage of 20v, (c) at an applied voltage of 35v, and (d) at an applied voltage of 45v. The amount of MWCNTs/PVA increases as voltage becomes higher. But there are apparent pores within the composite film for 45v.

Cyclic voltammetry (CV) is a highly effective method for probing the features of a surface-modified electrode using the redox probe $[Fe(CN)_6]^{3-/4-}$. Cyclic voltammograms obtained with different voltages of deposition in phosphate buffered solution (PBS) containing 1mM $K_3[Fe(CN)_6]$ at a scan rate of 10mv/s are shown in Fig.7 and from the CV curve a capacitance value could be generated, which can be characterized by integrating the areas under the curves. The anodic and catholic peak currents increase with increasing the voltage of EPD process. As more and more MWCNTs/PVA particles deposited on the substrate, the charge exchange rate on the surface of electrode is improved, and it explains why the current becomes higher with increasing voltage. For higher voltage (above 45v), as the electrolysis of water becomes severe, there are micropores dispersed among the deposit film and it may have a negative impact on the electrochemical property of modified electrode. That is why the peak current falls for 45 v deposition sample. And this phenomenon is consistent with the surface morphology of different kinds of MWCNTs/PVA -coated electrodes.

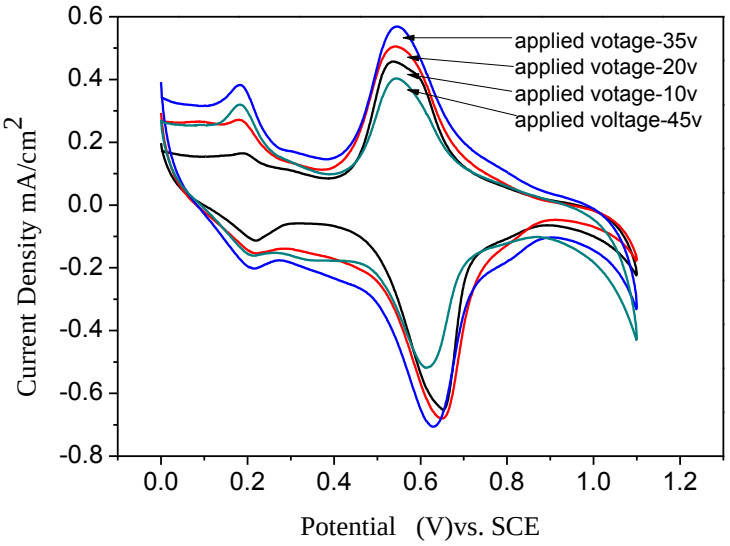

Figure 7. CV curves of 1 mM Fe $(CN)_6^{3-}$ in PBS for MWCNTs/PVA EPD processed electrodes at different applied voltages. The accumulation time and scan rate is 2s and 10mv/s, respectively. The electrochemical response of 35v applied voltage electrode is more prominent compared with others, for the oxidation and reduction peaks are sharper and the current is bigger.

3.2.3 Effect of time on deposit yield and electrochemical performance

The variation of deposit yield (Y) versus time (t) for deposition voltages of 35 V is shown in Figure 8(a). From 0.5 min to 2.5 min, the deposit yield increases with extending the time, and the tendency is matched with the theory. But as time prolonged, the phenomenon of electrolysis of water is also notable, and the bubbles near the surface of two electrodes affect the deposition process and then the deposit yield would not increase for longer time. So the deposition time should be limited within 2.5 min.

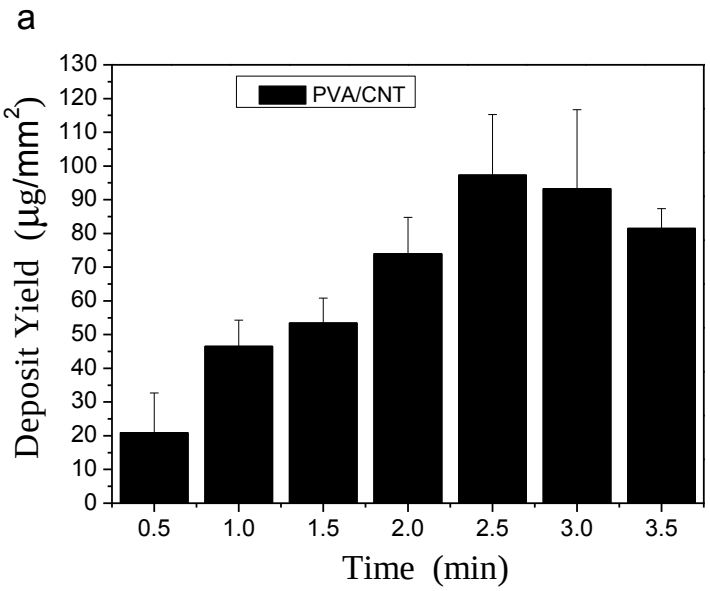

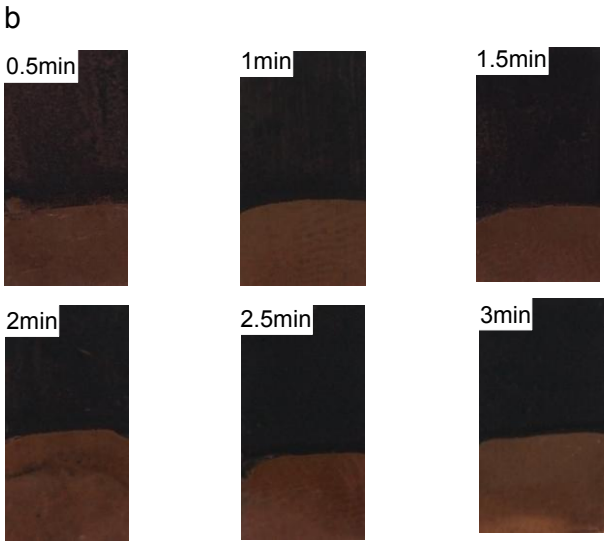

Figure 8 (a). Deposit yield versus deposition time for composite film prepared at a deposition voltage of 35 v. (b) Optical photographs of MWCNTs/PVA composite coating obtained by EPD for different time. As deposition time prolonged, deposit yield increases accordingly.

The macro surface morphology of deposits in Figure 8(b) may also prove this trend. Relationship between MWCNTs/PVA deposition yield and time for EPD is also verified by other researchers [43, 44].The surface morphology of different kinds of MWCNTs/PVA-modified electrodes corresponding to varied applied time is shown in Fig.9. From time 0.5min to 2.5min, the deposit density increases and the film becomes even; for 3.5min deposition, there are notable micropores.

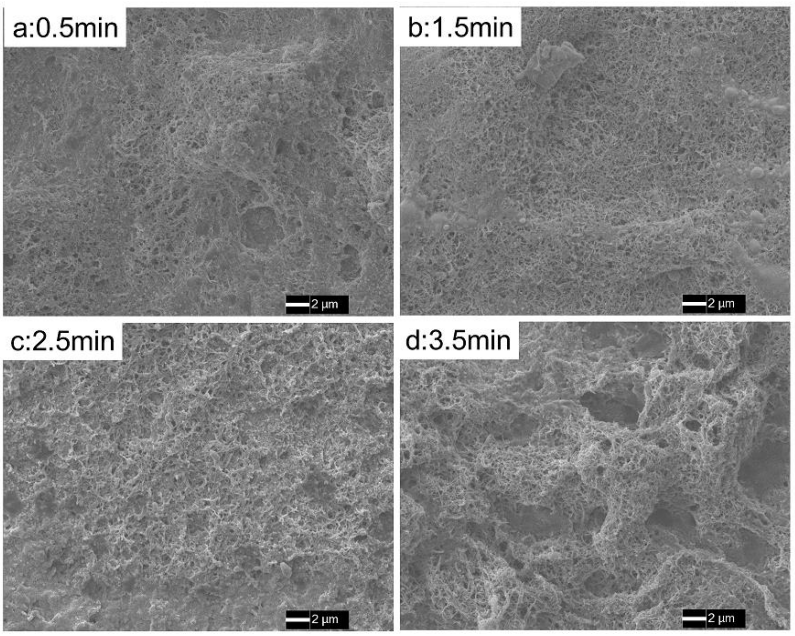

Figure 9. Surface morphology of composite film obtained by EPD for different deposition time (a) for 0.5min, (b) for 1.5min, (c) for 2.5min, and (d) for3.5min. The micropores caused by the electrolysis of water are notable within the composite film for the deposition time is 3.5min.

Cyclic voltammograms obtained with different time of deposition in PBS containing1mM K_3 [Fe (CN) $_6$] at a scan rate of 10mv/s are shown in Fig.10. The anodic and catholic peak currents increase with increasing the time of EPD process from 0.5min to 3min, but decrease for 3.5 min of deposition. This phenomenon is corresponding to the deposit yield vs. time curve and surface morphology of the electrodes. The more MWCNTs/PVA deposited on the electrode, the more active sites on modified electrode, and the response to the electron transfer is more sensitive. That explains the peak current increase with extending the time.

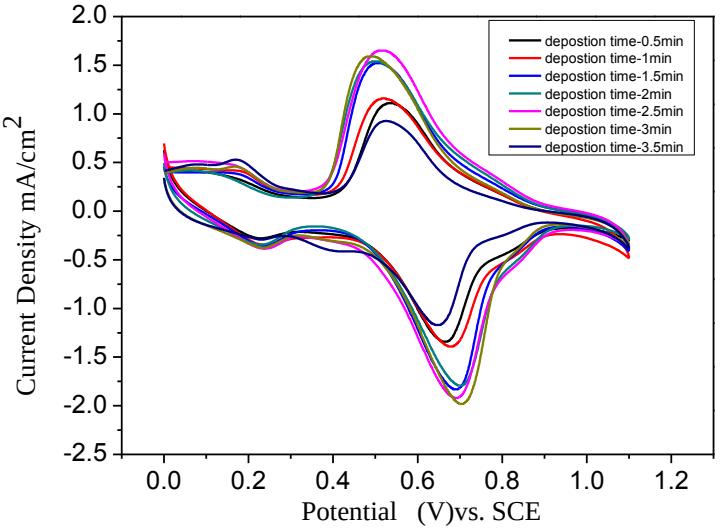

Figure 10. CV curves of 1 mM Fe (CN) $_6^{3-}$ in PBS for MWCNTs/PVA EPD processed electrodes for different deposition time. The accumulation time and scan rate is 2s and 10mv/s, respectively. The electrochemical response of 2.5 min deposition electrode is more prominent compared with others, for the oxidation and reduction peaks are sharper and the current is bigger.

3.3 Comparison between modified electrode and bare copper electrode

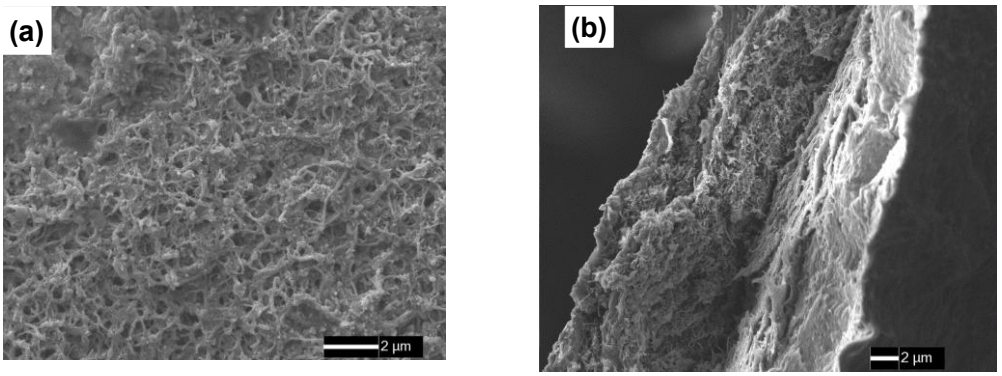

Figure 11. (a) Surface morphology of MWCNTs/PVA composite coating by electrophoretic deposition (b) Fracture surface of MWCNTs/PVA composite showing MWCNTs evenly embedded into the polymer matrix

After discussion about the effect of voltage and time on the electrochemical performance of electrode， optimal deposition condition is chosen at 35v for 2.5min. Fig11(a,b) shows the SEM images of MWCNTs/PVA composite coating on copper substrate at the applied potential of 35v and deposition time 2.5 min. Surface morphology of MWCNTs/PVA coating clearly depicts well dispersed MWCNTs throughout the polymer matrix. It manifested that proper applied voltage during EPD produced uniform and homogeneous deposit of controlled. The microstructural analysis of thin coating did not show any micro cracks. However, when the applied voltage is too high or the deposition time is prolonged, the quality of the composite coating is not desirable. Within short time and at a proper voltage, we got good uniform, homogenous, crack free deposition.The cyclic voltammograms obtained in phosphate buffered solution (PBS) containing1mM K_3 [Fe (CN) $_6$] at bare copper electrode and MWCNTs/PVA modified electrode at a scan rate of 10mv/s are shown in Fig.12 (a) that the redox peaks current: modified electrode > bare Cu. Oxidation and reduction peaks are observed at 0.643v and 0.566v at bare copper electrode, 0.624v and 0.542v at modified electrode. The peak-to-peak separation on copper is 77 mv, which is relatively close to the value obtained according to the theory and function. The peak to peak separation of MWCNTs/PVA modified electrodes is 82 mv and is slightly larger than copper which can be explained with the PVA film acting as a barrier against the Fe (CN) $_6^{3-}$ to reach the electrode surface, but the peaks current is much higher. This can be attributed to the larger electroactive surface area at the MWCNTs/PVA coating after the inclusion of MWCNTs in PVA matrices. It means due to the modification of MWCNTs, there are more active sites on the surface of the modified electrode, and the response to the electron transfer is more sensitive.

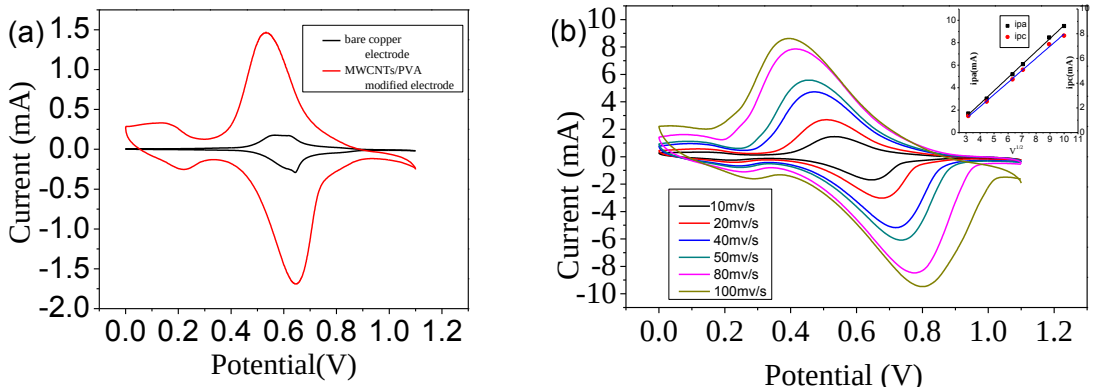

Figure 12. (a) Cyclic voltammetry responses of 1 mM Fe (CN) $_6^{3-}$ in PBS at bare copper electrode and MWCNTs/PVA modified electrode. (b) Cylic voltammograms at MWCNTs/PVA modified electrode in PBS containing 1 mM Fe (CN) $_6^{3-}$ at different scan rate. The insert shows the anodic and cathodic peak currents as a function of the square root of scan rate at MWCNTs/PVA modified electrode in PBS containing 1 mM Fe (CN) $_6^{3-}$

Cyclic voltammograms obtained with different scan rates in aqueous PBS containing 1mM Fe (CN) $_6^{3-}$at MWCNTs/PVA modified electrode are shown in Fig.12 (b). The anodic and cathodic peak currents increase with increasing the potential scan rate ranging from 10mV/s to 100mV/s. The

detailed description of the relationship between peak currents and scan rate is shown in the insert of Fig.12 (b). The anodic and cathodic peak current vs. square root of the scan rate is linear, which suggests that the process is predominantly diffusion controlled and manifests this type of modified electrode is much better when compared to bare copper electrode.

4. CONCLUSION

In this paper, we demonstrated a simple and efficient EPD method for co-depositing MWCNTs/PVA composite hydrogel coating on the copper substrate, using H_2O_2 and mixture of concentrated nitric and sulphuric acids to oxidize and electrostatically stabilize MWCNTs in water. How the zeta-potential of the MWCNTs/PVA composite particles in the solution influence the process of electrophoretic deposition has been discussed. As the local pH decreases near the anode as a matter of water electrolysis, the ζ-potential value reduced, which leads to the repulsive force among the particles becoming weak, and then the composite particles spontaneously coagulate to form deposition on the anode. The effect of main EPD parameters including applied voltage and deposition time on the deposit yield as well as electrochemical performance of modified electrode was investigated. The deposit yield increased by increasing applied voltage (below 35v) and deposit time (below 2.5min). This relationship was in good agreement with EPD theoretical relations considered for ceramic powders. The more MWCNTs/PVA deposited on the electrode, the more active sites on modified electrode, and the faster response to the electron transfer. By altering the parameters of deposition, different electrochemical properties were obtained. The optimized voltage and deposit time for EPD of MWCNTs/PVA composite hydrogel coating were found to be 35v and 2.5min. Based on the optimized process parameters, the novel MWCNTs/PVA modified electrode outperform bare copper electrode and the response to the electron transfer is more sensitive. Both anodic and cathodic peak currents of $Fe(CN)_6^{4-}$/ $Fe(CN)_6^{3-}$ redox system on modified electrode exceed those on bare copper electrode, which means there are more active sites on the surface of the modified electrode, and the response to the electron transfer is more sensitive when compared to bare copper electrode. This kind of composite coating can be easily applied to other metal substrate electrodes and this will further broaden the applications. The MWCNTs/PVA composite hydrogel coating modified electrode might be used in biosensors to investigate the biological systems.

ACKNOWLEDGEMENTS
This study is financially supported by National Natural Science Foundation of China Project (Grant No.51073024 and Grant No. 51273021), the Royal Society-NSFC International Joint Project (Grant No.51111130207), and the National Science and Technology Support Project of China (Grant No. 2011BAK15B04).

References

1. C. Wang, J. Ma and W. Cheng, *Surf. Coat. Technol*., 173 (2003) 271.

2. A.R. Gardeshzadeh and B. Raissi, *Prog. Color Colorants Coat*., 4 (2011) 51.
3. H. Ogihara, M. Fukasawa and T. Saji, *Carbon*, 49 (2011) 4604.
4. C. Kaya, I. Singh and A.R. Boccaccini, *Adv. Eng. Mater*., 10 (2008) 131.
5. K. Wu, P. Imin, Y. Sun, X. Pang, A. Adronov and I. Zhitomirsky, *Mater. Lett*., 67 (2012) 248.
6. Y. Wang, I. Deen and I. Zhitomirsky, *J. Colloid Interface Sci*., 362 (2011) 367.
7. F. Sun and I. Zhitomirsky, *Surf. Eng*., 25 (2009) 621.
8. M. Cheong and I. Zhitomirsky, *Colloid. Surface.* A., 328 (2008) 73.
9. L. Besra, T. Uchikoshi, T.S. Suzuki and Y. Sakka, *J. Eur. Ceram. Soc*., 30 (2010) 1187.
10. A.R. Boccaccini, S. Keim, R. Ma, Y. Li and I. Zhitomirsky, *J. R. Soc. Interface., 7* (2010) S581.
11. Y. Wang, X. Pang and I. Zhitomirsky, *Colloid. Surface*. B., 87 (2011) 505.
12. J.J. Gooding, R. Wibowo, Liu, W. Yang, D. Losic, S. Orbons, F.J. Mearns, J.G. Shapter and D.B. Hibbert, *J. Am. Chem. Soc.*, 125 (2003) 9006.
13. F. Patolsky, Y. Weizmann and I. Willner, *Angew. Chem. Int. Edit.*, 43 (2004) 2113.
14. J. Rusling, X. Yu, B. Munge, V. Patel, G. Jensen, A. Bhirde, J. Gong, S. Kim, S. Gutkind and F. Papadimitrakopoulos, *ECS Meeting Abstracts*, 602 (2006) 716.
15. S. Minnikanti, P. Skeath and N. Peixoto, *Carbon*, 47 (2009) 884.
16. P.J. Britto, K.S.V. Santhanam and P.M. Ajayan, *Bioelectrochemistry*, 41 (1996) 121.
17. J.J. Davis, R.J. Coles, H. Allen and O. Hill, *J. Electroanal. Chem*., 440 (1997) 279.
18. F. Valentini, A. Amine, S. Orlanducci, M.L. Terranova and G. Palleschi, *Anal. Chem.*, 75 (2003) 5413.
19. Y.-C. Tsai and J.-D. Huang, *Electrochem. Commun*., 8 (2006) 956.
20. P.A. Tran, L. Zhang and T.J. Webster, *Adv. Drug Delivery Rev*., 61 (2009) 1097.
21. A. Peled, E. Zaguri and G. Marom, *Compos. Part A-Appl* S., 39 (2008) 930.
22. A. Nilasaroya, L.A. Poole-Warren, J.M. Whitelock and P. Jo Martens, *Biomaterials*, 29 (2008) 4658.
23. M.L. Minus, H.G. Chae and S. Kumar, *Macromol. Chem. Phys*., 210 (2009) 1799.
24. R. Ma, D. Xiong, F. Miao, J. Zhang and Y. Peng, *Mater. Sci. Eng*. C, 29 (2009) 1979.
25. H. Bodugoz-Senturk, C.E. Macias, J.H. Kung and O.K. Muratoglu, *Biomaterials*, 30 (2009) 589.
26. S. Bhattacharyya, S. Guillot, H. Dabboue, J.-F. Tranchant and J.-P. Salvetat, *Biomacromolecules*, 9 (2008) 505.
27. S. Chatterjee, M.W. Lee and S.H. Woo, *Carbon*, 47 (2009) 2933.
28. K.Y. Lee and D.J. Mooney, *ChemInform*, 32 (2001) no.
29. E.F.d.l. Cruz, Y. Zheng, E. Torres, W. Li, W. Song and K. Burugapalli, *Int. J. Electrochem. Sci.*, 7 (2012) 3577.
30. Y. Huang, Y. Zheng, W. Song, Y. Ma, J. Wu and L. Fan, *Compos. Part A-Appl* S., 42 (2011) 1398.
31. Y.X. Ma, Y.D. Zheng, J. Wu, J. Tan, W. Li and Y. Yu, *Adv. Mater. Research*, 236 - 238 (2011) 1832.
32. Z. Liu, Z. Shen, T. Zhu, S. Hou, L. Ying, Z. Shi and Z. Gu, *Langmuir*, 16 (2000) 3569.
33. J.D. Gong, G. Jensen, A. Bhirde, Y. Xin, B. Munge, V. Patel, K. Sang Nyon, J. Silvio Gutkind, F. Papadimitrakopoulos and J.F. Rusling, in: Wearable and Implantable Body Sensor Networks, 2006. BSN 2006. International Workshop on, (2006) 5.
34. J. Ming, Y. Wu, Y. Yu and F. Zhao, *Chem. Commun*., 47 (2011) 5223.
35. P. He and L. Dai, Carbon Nanotube Biosensors, in: M. Ferrari, A.P. Lee, andL.J. Lee (Eds.) BioMEMS and Biomedical Nanotechnology, Springer US, 2006(171).
36. H.E. Ries, Nature, 226 (1970) 72.
37. L. Jiang, L. Gao and J. Sun, *J. Colloid Interface Sci.*, 260 (2003) 89.
38. F. Grillon, D. Fayeulle and M. Jeandin, *J. Mater. Sci. Lett*., 11 (1992) 272.
39. I. Zhitomirsky, *Sci Adv. Colloid Interface Sci*., 97 (2002) 279.
40. J. Cho, K. Konopka, K. Rożniatowski, E. García-Lecina, M.S.P. Shaffer and A.R. Boccaccini, *Carbon*, 47 (2009) 58.

41. H.C. Hamaker, *Trans. Faraday Soc*., 35 (1940) 279.
42. J. Cho, K. Konopka, K. Rozniatowski, E. García-Lecina, M.S.P. Shaffer and A.R. *Boccaccini, Carbon*, 47 (2009) 58.
43. L. Besra and M. Liu, *Prog. Mater. Sci*., 52 (2007) 1.
44. L. Besra, T. Uchikoshi, T.S. Suzuki and Y. Sakka, *J. Eur. Ceram. Soc*., 29 (2009) 1837.